OPEN

Citation: Blood Cancer Journal (2013) 3, e106; doi:10.1038/bcj.2013.4

www.nature.com/bcj

ORIGINAL ARTICLE

Efficacy of an adapted granzyme B-based anti-CD30 cytolytic fusion protein against PI-9-positive classical Hodgkin lymphoma cells in a murine model

S Schiffer[1,2], HP Hansen[3], G Hehmann-Titt[4], M Huhn[1], R Fischer[2], S Barth[1,2,5] and T Thepen[2,5]

Tumors develop when infiltrating immune cells contribute growth stimuli, and cancer cells are selected to survive within such a cytotoxic microenvironment. One possible immune-escape mechanism is the upregulation of PI-9 (Serpin B9) within cancer cells. This serine proteinase inhibitor selectively inactivates apoptosis-inducing granzyme B (GrB) from cytotoxic granules of innate immune cells. We demonstrate that most classical Hodgkin lymphoma (cHL)-derived cell lines express PI-9, which protects them against the GrB attack and thereby renders them resistant against GrB-based immunotherapeutics. To circumvent this disadvantage, we developed PI-9-insensitive human GrB mutants as fusion proteins to target the Hodgkin-selective receptor CD30. In contrast to the wild-type GrB, a R201K point-mutated GrB construct most efficiently killed PI-9-positive and -negative cHL cells. This was tested *in vitro* and also *in vivo* whereby a novel optical imaging-based tumor model with HL cell line L428 was applied. Therefore, this variant, as part of the next generation immunotherapeutics, also named cytolytic fusion proteins showing reduced immunogenicity, is a promising molecule for (targeted) therapy of patients with relapsing malignancies, such as cHL, and possibly other PI-9-positive malignancies, such as breast or lung carcinoma.

Blood Cancer Journal (2013) **3,** e106; doi:10.1038/bcj.2013.4; published online 22 March 2013

Keywords: targeted cancer therapy; serine protease; treatment resistance; Serpin B9; immunotoxin

INTRODUCTION

A major problem of conventional cancer therapy is its lack of specificity. Thus, more specific approaches are now under investigation to exclusively kill abnormal cells. One of the strategies comprises the development of immunotoxins, which consist of a cell-binding moiety and a cell death-inducing agent. As plant- or bacteria-derived toxins can cause severe side effects, the generation of less immunogenic compounds is essential. This led to the fourth generation of immunotoxins, first so coined by Mathew and Verma,[1] which include humanization of both the cell-binding ligand as well as the pro-apoptotic enzyme. Owing to the high effectiveness and importance of granzymes during the immune response of humans, these serine proteases are promising candidates for the development of antitumor immunotherapies. The best studied and the most promising one is granzyme B (GrB),[2–8] an effector molecule stored in the granules of cytotoxic immune cells to kill transformed tumor or virus-infected cells.[9,10] However, its antitumoral efficacy is limited by irreversible inhibition by PI-9. PI-9 is co-expressed in the cytosol of cytotoxic immune cells to avoid autotoxicity in case of granule leakage of misdirected GrB. Several tumors have also been described to express PI-9, such as breast cancer,[11] metastasizing melanoma,[12] lung cancer[13] and prostate cancer,[14] and also classical Hodgkin lymphoma (cHL) is a typical example for this phenomena.[15] It has been shown that PI-9 expression is heterogeneous within the tumor cell population. As a very high number of positive tumor cells predict unfavorable clinical outcome, these might be positively selected upon immune surveillance.[12,16] Killing these treatment-resistant cells may therefore strongly increase the therapeutic success and possibly lifespan. Therefore, we recently generated a variety of GrB mutants, which showed a reduced PI-9-inhibitor binding in the first experimental studies.[17] Here, we introduce a novel GrB-based antitumor approach targeting the cHL receptor CD30. As animal model for HL, only L540cy cells are established so far. In addition, based on the recently suggested optical-imaging technique,[18] we here describe a novel tumor model with the cHL cell line L428. Subsequently, we were able to compare the cytotoxic efficacy of cytolytic fusion proteins (CFPs) using four different GrB point mutations[17,19] in the PI-9-binding site of GrB not only *in vitro* but also *in vivo*. In this study, the R201K GrB mutant demonstrated the best antitumor efficacy against both PI-9-positive and -negative tumor cells.

MATERIALS AND METHODS

Protein preparation

The pMS plasmid encoding EGb-H22(scFv)[20] was used to construct EGb-Ki4(scFv) by replacing the coding sequence for the single chain variable fragment H22(scFv)[6] by Ki4(scFv).[21] Mutations were inserted with specific primers via site-directed mutagenesis by overlap extension.[17] The construct (Figure 1a) includes an enterokinase site, enabling the activation of GrB[22] and an IGκ leader sequence for secretory expression.[20] Secretory mammalian expression in HEK293T cells and purification via affinity

[1]Department of Experimental Medicine and Immunotherapy, RWTH Aachen, Helmholtz Institute for Biomedical Engineering, Aachen, Germany; [2]Department of Pharmaceutical Product Development, Fraunhofer Institute for Molecular Biology and Applied Ecology IME, Aachen, Germany; [3]Department I of Internal Medicine, University Clinic Cologne, Cologne, Germany and [4]Pharmedartis GmbH, Aachen, Germany. Correspondence: Professor S Barth, Department of Pharmaceutical Product Development, Fraunhofer Institute for Molecular Biology and Applied Ecology IME, Forckenbeckstr 6, Aachen 52074, Germany.
E-mail: stefan.barth@ime.fraunhofer.de
[5]These authors contributed equally to this work.
Received 30 November 2012; revised 13 February 2013; accepted 13 February 2013

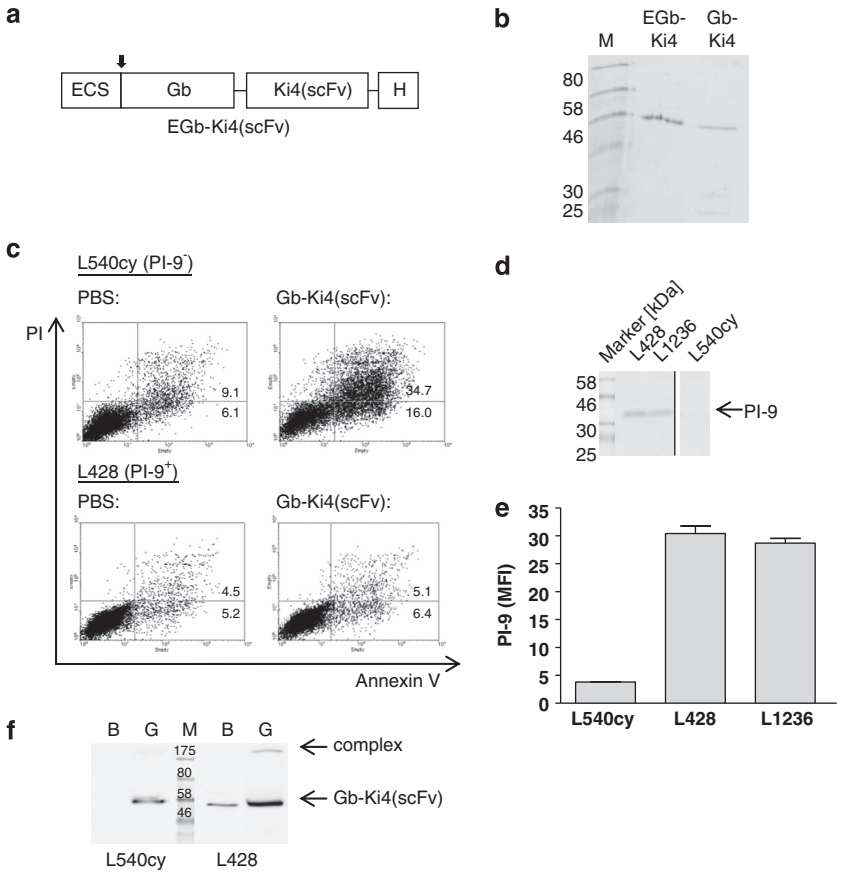

Figure 1. (**a**) Schematic structure of the protein EGb-Ki4(scFv). After purification, it is activated via enterokinase ('E')-digestion site indicated by an arrow. (**b**) Coomassie-stained SDS-PAGE gel with purified Gb-Ki4(scFv) before and after activation with enterokinase. (**c**) Results of apoptosis assay (annexin V/propidium iodide staining) on PI-9$^-$ L540cy cells and PI-9$^+$ L428 cells after incubation with 33 nM Gb-Ki4(scFv). Numbers are % of cells within corresponding quadrant. (**d** and **e**) Expression of PI-9 in cHL cell lines L428, L1236 and L540cy. (**d**) Total soluble protein (40 μg/lane) was loaded on a gel for SDS-PAGE, and PI-9 was subsequently detected in a western blot using the antihuman PI-9 (clone 7D8) and GAM-PO. (**e**) 1×10^6 cells, as indicated, were fixed, permeabilized and stained with antihuman PI-9 (7D8) and GAM-FITC. PI-9 expression was determined by flow cytometry. (**f**) Complex formation of PI-9 and Gb-Ki4(scFv) within cell lysates of L540cy and L428 cells after pre-incubation with Gb-Ki4(scFv) 'G' or buffer 'B'. Altogether, 40 μg total soluble protein was loaded on SDS-gel, and western blot was analyzed with antihuman GrB. Unspecific band was detected on the same height of CFP.

chromatography of EGb-Ki4(scFv) and its mutants were done as described previously.[6]

Cell lines

The cHL cell lines L540cy,[23] L428 (DSMZ, ACC 197), L1236 (DSMZ, ACC 530), the AML cell line HL60 (DSMZ, ACC-3) and the Human Embryonic Kidney cell line HEK293T (ATCC, CRL-11268) were cultivated in RPMI 1640 plus Gluta-MAX-I, including 10% (v/v) fetal calf serum, 100 μg/ml penicillin and streptomycin at 37 °C, and 5% CO_2. Altogether, 100 μg/ml Zeocin was added to the transfected HEK293T cells for selection purposes.

Protein characterization

Enzymatic activity. The proteolytic activity of 100 nM Gb-Ki4(scFv) and GbR201K-Ki4(scFv) after enterokinase digestion was detected by cleavage of 200 μM of the synthetic substrate Ac-IETD-*p*NA (Calbiochem/Merck, Darmstadt, Germany) which mimicks the cleavage site of pro-caspase 3. The reaction was monitored in an ELISA plate reader (BioTek Instruments, Epoch, Bad Friedrichshall, Germany) at 405 nm and 37 °C for 60 min in a 2-min interval.

Binding. The binding of Gb-Ki4(scFv) and its mutants to L428 was evaluated via flow cytometric analysis (CellQuest Version 3.3 (Becton Dickinson, Heidelberg, Germany)) and WinMDI 2.8, (The Scripps Institute, West Lafayette, IN, USA). A total of 4×10^5 cells were washed with PBS and incubated with 1 μg purified protein in 100 μl PBS for 30 min on ice. After washing, cells were incubated with anti-His Alexa 488 for 30 min on ice in the dark. The CD30-negative HL60 cell line was used as a negative control. For the determination of the affinity constant K_d, different concentrations of Gb-Ki4(scFv) or GbR201K-Ki4(scFv) were incubated with target cells L428 and L540cy. Mean fluorescence intensities were evaluated via WinMDI 2.8 and compared by non-linear-regression determinations in GraphPad Prism 4.0, La Jolla, CA, USA.

Serum stability. A total of 70 ng/μl purified protein was incubated with 50% murine serum at 37 °C for different time periods between 0 and 48 h. Remaining protein binding activity was measured via flow cytometric analysis as described elsewhere,[24] here with 400-fold dilution of 7.5 μl of the mixture.

Internalization determination

Ki4(scFv)-SNAP protein was produced by secretory expression of HEK293T cells as described above for Gb-Ki4(scFv), and coupled to Alexa-Fluor-BG-647 according to the manufacturer's instructions (NEB). In order to verify internalization, 4×10^5 cells were incubated at 4 or 37 °C, respectively, for 2 h with 1 μg Ki4(scFv)-SNAP-BG-647 in 300 μl PBS or only in PBS as negative control. After washing of the cells, antigen-dependent internalization was detected by confocal laser-scanning microscopy (TCS SP5).

Detection of endogenous PI-9 and GrB-PI-9 complex

Cells were lysed with PBS containing 1% Triton X-100. Endogenous PI-9 was detected by western blot or flow cytometry using the antibodies antihuman PI-9 (clone 7D8, Santa Cruz Biotechnology, Santa Cruz, CA, USA) and GAM-PO or GAM-FITC (Sigma-Aldrich, Taufkirchen, Germany), respectively. Signal detection on western blots was done by

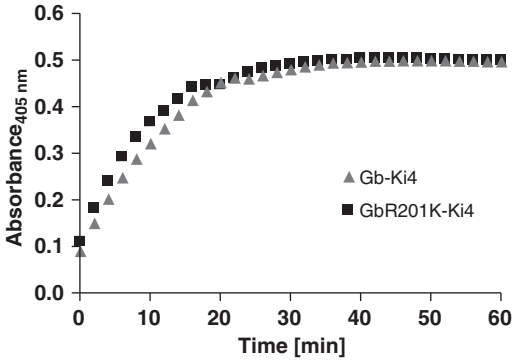

Figure 2. Enzymatic activity of Gb-Ki4(scFv) and its mutant GbR201K-Ki4(scFv) determined via a colorimetric assay based on the synthetic GrB substrate Ac-IETD-*p*NA. Absorbance at 405 nm was monitored in a 2-min interval for 60 min at 37 °C. Activities for both constructs were the same.

chemiluminescence detection system (Leica LAS-3000, Fujifilm, Duesseldorf, Germany). Mean fluorescence intensities were evaluated by flow cytometry and WinMDI 2.8.

Endogenous complex formation was determined after incubation with Gb-Ki4(scFv) as described for apoptosis assay. Analysis was done as above using antihuman GrB (clone 2C5, Santa Cruz) and GAM-PO.

Cytotoxicity assays

A total of 2×10^5 cells were incubated for 48 h either with 11 nM or with different dilutions of CFP in 12-well-plates, if not otherwise indicated.

Viability. For subsequent dose-depending evaluation of viability, the metabolic activity of cells towards tetrazolium salt XTT was applied according to the manufacturer's instructions (Serva, Heidelberg, Germany).

Toxicity. For apoptosis assay after incubation with CFPs, annexin V-GFP and propidium iodide were added to the washed cells as described before.[6] Dead cells and early and late apoptotic cells were detected by flow cytometry. The buffer control was assigned a viability of 100% and treated samples were converted accordingly.

Caspase 3/7. In order to determine the caspase 3/7 activity a preluminescent caspase 3/7-DEVD-aminoluciferine substrate (Caspase-Glo 3/7 Assay, Promega GmbH, Mannheim, Germany) was added to the treated cells. The measured luminescence signal is directly proportional to the activity of caspase 3/7 and was normalized to the background signal produced by Gb-Ki4(scFv).

Biological activity of selected CFPs *in vivo*

Animal experiments were approved by the local Animal Care and Use Review Committee. A total of 5×10^6 L428 cells transfected with the FR fluorescent protein, Kat2,[18] (pTag-Katushka2-N; Evrogen, Moscow, Russia) or L540cy (not transfected), resuspended in 50% Matrigel (growth factor-reduced; BD Bioscience, Heidelberg, Germany), were injected subcutaneously into the right hindlimb of 8-week-old female BALB/c nu/nu mice (Charles River, Germany). Tumor growth was monitored by molecular imaging with the CRi Maestro system (Cri Inc, Woburn, MA, USA) for L428 as described before[18] ($n = 7$ per group); for L540cy ($n = 6$ for GbR201K-Ki4(scFv), $n = 3$ for GbR201K-H22(scFv)) triplet caliper measurements were done. Treatment schedules are shown in Figures 5a and 6a. Targeting of $CD30^+$ L540cy cells with Ki4(scFv)-SNAP-BG-747 was done according to published protocols.[25] Tumors were resected from sacrificed animals and cut into 8-μm sections on a freezing microtome. After drying, tissue slices were stained with Ki4(scFv)-SNAP-BG-Vista-Green and signals visualized via confocal microscopy (Leica, TCS SP5).

Statistics

Statistical analysis was done by two-tailed *t*-test using GraphPad Prism 4.0; $P < 0.05$ was considered to be statistically significant.

RESULTS AND DISCUSSION

GrB is one of the most potent and well-established effector molecules having the highest potential for targeted antitumor therapy due to the human origin of its enzymatic activity. This minimizes unwanted immune reactions in patients related to CFPs. Their potential has been shown in tumor cell lines that are resistant against cytotoxic drugs. However, its efficacy is diminished by the endogenous inhibitor PI-9 that can be expressed by tumors as escape mechanism. This expression correlates with unfavorable prognosis for the patients, so that a specific killing of those cells could be beneficial and the development of PI-9-resistant GrB-based CFPs could meet this demand. On the down side, such alterations may introduce novel sequences with potential antigenicity.

We fused GrB to the CD30 targeting murine Ki4(scFv), which is the anti-CD30 single chain of choice, due to its property of not binding the shed CD30 receptor.[26] This is important as it has been reported that CD30 ectodomain shedding occurs at high incidences,[27] which could lead to an off-target capturing of the CFP. We selected cHL and used the receptor CD30 as target in a proof-of-principle model because it has already been successfully used in CFP-based approaches, for example, by Brentuximab–Vedotin[28] or Ki4(scFv)-ETA.[21] The mammalian expression of our constructs that results in natural glycosylation patterns of GrB was successful. To obtain the enzymatically active protein Gb-Ki4(scFv), EGb-Ki4(scFv) had to be activated by enterokinase. The purified protein before and after enterokinase digestion is shown in Figure 1b. Proteolytic activity was verified via colorimetric substrate assay, whereby no differences between the kinetics of wild-type Gb-Ki4(scFv) versus its mutant GbR201K-Ki4(scFv) were observed (Figure 2). The comparative enzymatic activities of all the generated mutants have been published earlier and indicate no significant difference between the mutants and the wild type described here.[17]

cHL represents a typical disease for the application of CFPs, as despite of high cure rates, 15–30% of the cHL patients relapse after conventional therapy, and this is associated with poor prognosis. This treatment resistance can be due to tumor-escape mechanisms like induction of PI-9 or downregulation of the CD30 receptor. During an initial apoptosis assay, we observed a limited effect of wild-type Gb Ki4(scFv) on L428 cell line, whereas successful induction of cell death was seen on L540cy cells (Figure 1c). As marked differences in CD30 receptor expression were observed (Figure 3c) and to assure that cytotoxic differences were not due to subsequent diminished internalization, we tested internalization of Ki4(scFv)-SNAP-BG-647 as described earlier.[25] Thereby, we observed complete internalization after 2 h at 37 °C (Figure 3d), so that the described effect could be excluded. Only External binding was observed after incubation at 4 °C, excluding unspecific internalization. After lysing the cells following treatment with Gb-Ki4(scFv) analysis by western blot with a GrB-specific antibody, we observed an additional high-running band within the probe derived from Gb-Ki4(scFv)-treated L428 cells, which was absent in the one of L540cy (Figure 1f). As shown before, this could be interpreted as the SDS-stable complex between PI-9 and Gb-Ki4(scFv).[29] At the same time and in spite of the non-specifically detected band at the same expected height of Gb-Ki4(scFv) within the buffer control, we could thereby verify the successful internalization of the CFP. Additionally, via western blot and flow cytometric analysis, we demonstrated that the HL cell lines differ in their PI-9 expression. Therefore, the T-typed L540cy lacked PI-9, whereas the B-typed cells, L1236 and L428, showed a strong expression (Figures 1d and e). These findings are in accordance with an earlier study showing that 10% of all tested HL patients ($n = 57$) expressed the inhibitor.[15] In addition, this expression was also found upon Epstein–Barr virus infection, which is a major cause of B-type HL[30] and was recently even directly linked to Epstein–Barr virus-positive cases of HL.[31]

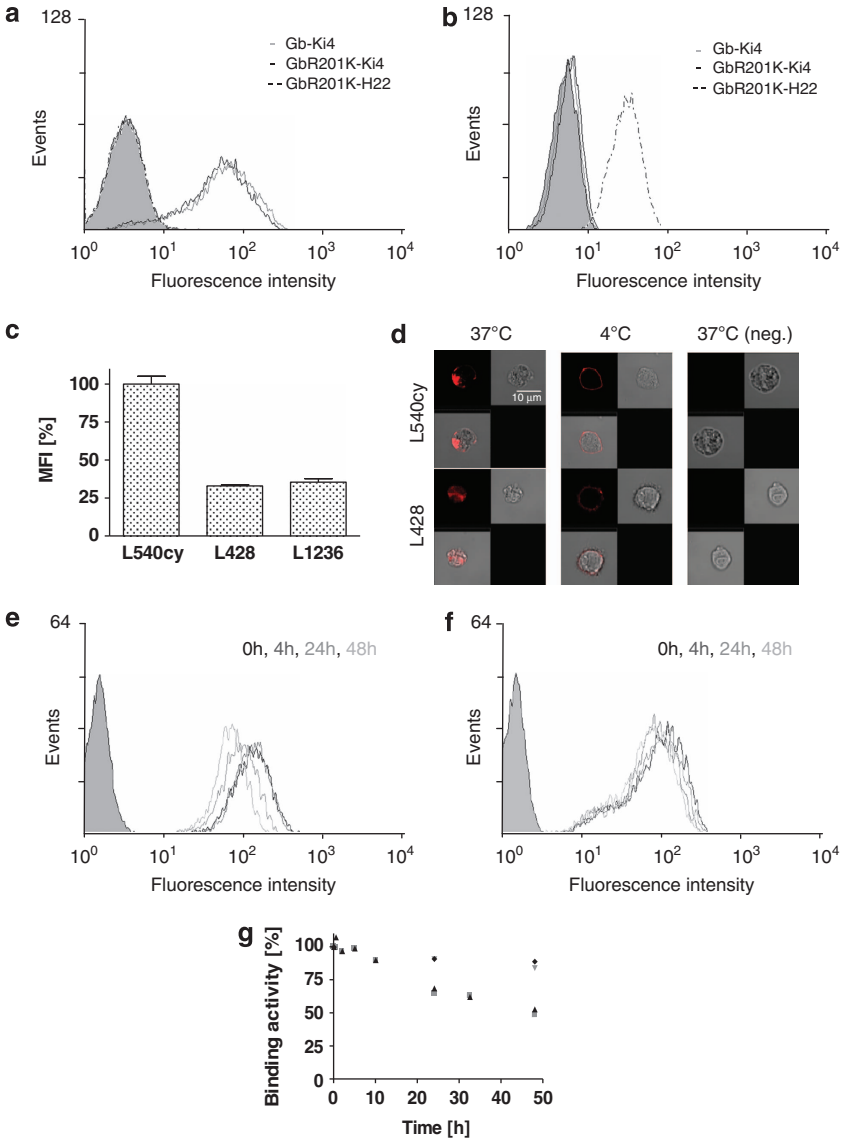

Figure 3. (**a** and **b**) Flow cytometric binding analysis of Gb-Ki4(scFv), GbR201K-Ki4(scFv) and GbR201K-H22(scFv) to CD30$^+$ target cell line L428 (**a**), and to CD30$^-$ cell line HL60 (AML) (**b**). Gray background is second antibody control. (**c**) Comparison of mean fluorescence intensities after binding of Gb-Ki4(scFv) to cell lines. MFI values correlate with CD30 surface expression. Shift for L540cy was set to 100%. (**d**) Confocal microscopy of CD30$^+$ cell lines, L540cy and L428, after incubation with Ki4(scFv)-SNAP-BG-647 at 37 and 4 °C. Negative control is incubated only in buffer. Internalization was analyzed after 2-h incubation. Serum stability of the CFPs for at least 10 h was confirmed by residual binding activity to L540cy, measured via flow cytometry after different incubation times in 50% mouse serum (**e**), or PBS (**f**). Data shown for GbR201K-Ki4(scFv). (**g**) Overview of serum stability based on MFIs measured during flow cytometric analysis shown in % of MFI related to 0 h. Data in gray for Gb-Ki4(scFv) (triangle: PBS, rectangle: serum) and in black for GbR201K-Ki4(scFv) (triangle: serum, rectangle: PBS). Representative data from one out of three experiments are shown.

As mentioned earlier, PI-9-insensitive GrB candidates were generated and published previously, their applicability and efficacy on cells *in vitro* and *in vivo*, however, remained to be established.[17] Here, the three most promising candidates: R28K, R201A and R201K and an additional one previously described in literature, K27A,[19] were compared with the wild-type protein for binding activity and affinity to target cells and serum stability of the protein. Results are shown for the best mutant R201K. As exemplary shown for cell line L428 in Figures 3a and b, both wild type and mutant specifically bind to the target cells and do not exhibit unspecific binding to a CD30-negative cell line, HL60. The affinity constants K_d were 3.6 nM on L540cy and 1.5 nM on L428 for Gb-Ki4(scFv), and 5.7 nM and 1.9 nM for GbR201K-Ki4(scFv), respectively. Additionally, their serum stability was compared to the stability in buffer (Figures 3e–g). A sufficient stability for at least 10 h in serum could be confirmed for both constructs. Next, we tested the cytotoxic activity of the mutants in comparison to the wild-type CFP on the PI-9-negative cell line L540cy. The observed IC_{50} values were all in the same range between 1.7 and 5.1 nM (Figure 4a). To confirm apoptosis induction, we performed an annexin V assay depicted in Figure 4b, with normalized data converted to viability. From the data, it could be concluded that the point mutations did not alter stability, binding affinity or cytotoxicity towards PI-9-negative cells of Gb-Ki4(scFv).

Based on the initial studies indicating a decreased apoptotic effect of Gb-Ki4(scFv) due to the expression of endogenous PI-9 (Figures 1c and f), we compared the *in vitro* antitumor efficacy of the four GrB mutants in PI-9-positive cells (Figures 4c). The most effective one, R201K, reduced the viability in both PI-9-positive (L428, L1236) and PI-9-negative (L540cy) cell lines, resulting in

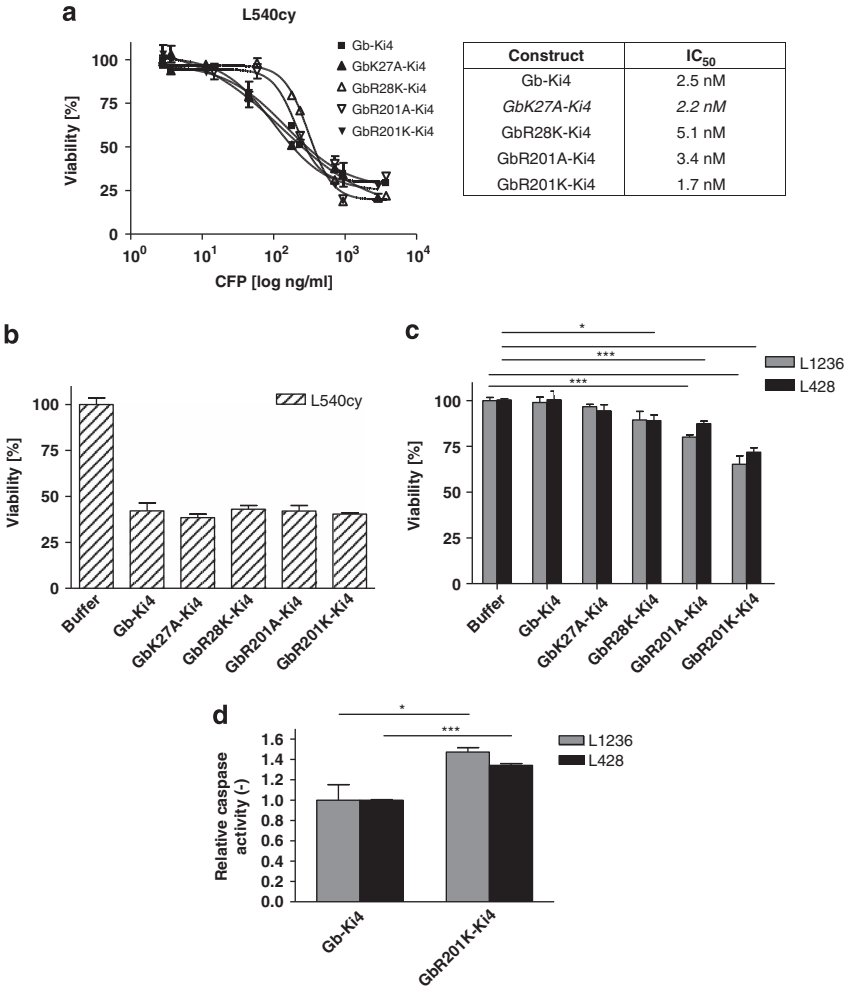

Construct	IC_{50}
Gb-Ki4	2.5 nM
GbK27A-Ki4	*2.2 nM*
GbR28K-Ki4	5.1 nM
GbR201A-Ki4	3.4 nM
GbR201K-Ki4	1.7 nM

Figure 4. (**a**) Colorimetric cytotoxicity assays with various CFP concentrations ($n = 3$ parallel cell cultures per dilution) showing strong dose-dependent effects of Gb-Ki4(scFv) and its mutants on $PI9^-$ L540cy. IC_{50} values are listed for all constructs. (**b** and **c**) Toxic effect of 11 nM Gb-Ki4(scFv) variants in 2×10^5 L540cy cells (**b**; $PI\text{-}9^-$) and L1236 and L428 (**c**; $PI\text{-}9^+$) after 48 h of cultivation at 37 °C. (**b**) Apoptotic cells were determined via normalized annexin V-GFP flow cytometric analysis and converted to viability. The statistical significance between treated and untreated samples was $P < 0.005$. (**c**) Viability was determined by XTT metabolization. Standard deviations are shown for three–five independent experiments. All statistical significances were determined via two-tailed *t*-test: (*) for $P < 0.05$ and (***) for $P < 0.001$. (**d**) Successful activation of caspase 3/7 by the mutated construct GbR201K-Ki4(scFv) in $PI\text{-}9^+$ L428 and L1236 was demonstrated via a preluminescent caspase 3/7-DEVD-aminoluciferine substrate. Data are shown as normalized to the background signal of Gb-Ki4(scFv).

62% viability in L1236, 70% in L428 and 40% in L540cy compared with the untreated control ($P < 0.001$). The strong differences in apoptosis between the L540cy on one hand, and the L1236 and L428 on the other hand induced by all constructs used (compare Figures 4b and c, respectively) can be explained by the published, lower overall sensitivity for apoptosis induction by the latter two.[32,33] Moreover, the PI-9-positive, CD30-expressing chronic myeloid leukemia cell line, K562,[34] showed a differential effect to the wild type and mutant in apoptosis induction. Here, 58% of the cells were killed by GbR201K-Ki4(scFv), whereas the wild-type did not induce cell death at all (data not shown). We could further verify our results by a statistically significant increase of caspase 3/7 activity (Figure 4d), an indicator of apoptosis induction, within the PI-9-positive cells after incubation with GbR201K-Ki4(scFv), in contrast to the treatment with Gb-Ki4(scFv), which only produced the expected background signal. The wild-type and the already published mutant K27A were effective in PI-9-negative cells only.

In vivo studies for cHL have so far been strongly restricted, as the only cell line that sufficiently grows in mice is L540 or L540cy. PI-9-positive L428 cells only grow slowly and transiently in mice so that caliper measurement of tumor size is impossible. However, by Kat2-transfection of these cells, we were nevertheless able to monitor tumor growth by optical imaging. In this subcutaneous tumor model, the therapeutic efficacy of the wild-type Gb-Ki4(scFv) and its best mutant GbR201K-Ki4(scFv) were compared. GbR201K-H22(scFv) was used as a non-binding control. Only the mutant was able to kill PI-9-positive cells *in vivo*. Here, the tumor size reduction was statistically significant compared with both wild type ($P < 0.05$) and control ($P < 0.005$), whereas the difference between the determined relative tumor size for the wild-type treated and the control group were not statistically significant (Figure 5b).

No difference in cytotoxic activity between Gb Ki4(scFv) and its mutant R201K was detected on PI-9-negative cells *in vitro*, therefore, only the mutant was used to confirm its effectiveness on PI-9-negative cells *in vivo*. Treatment with GbR201K-Ki4(scFv) triggered an arrest of tumor growth, whereas tumors in mice receiving non-binding GbR201K-H22(scFv) increased to over 100% of the original size (mm^2) ($P < 0.001$, Figure 6b).

Therefore, in contrast to the GrB wild type, our newly developed mutant GbR201K-Ki4(scFv) was able to kill both PI-9-positive and -negative tumor cells *in vitro* as well as *in vivo*.

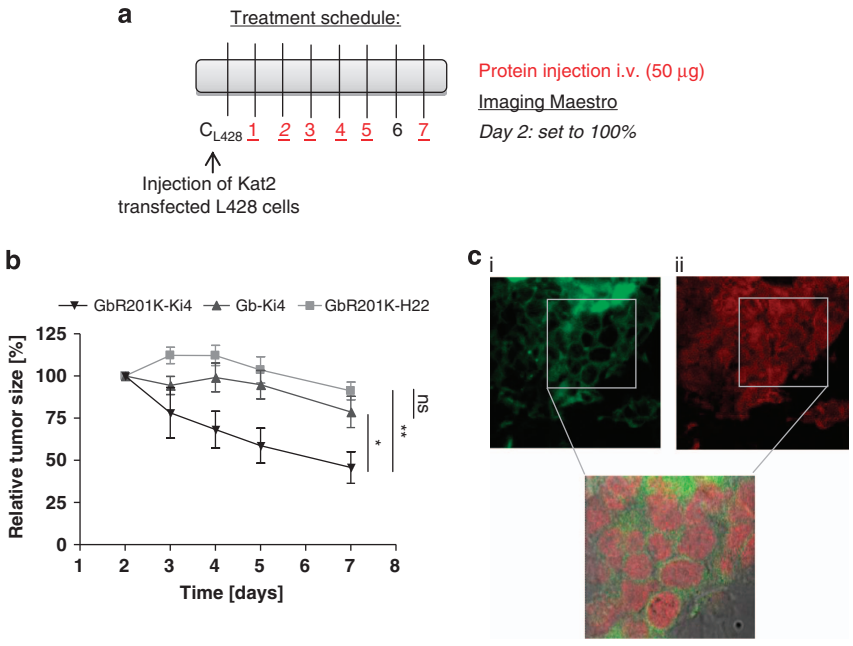

Figure 5. Results of mouse experiments with L428-induced tumors. (**a**) Treatment schedule indicating intravenous (i.v.) injection of L428 cells, protein injection and days of measurement. (**b**) Relative tumor size after treatment with fusion proteins, as indicated. Tumor size was estimated by imaging with the Cri Maestro System. The mutant GbR201K-Ki4(scFv) caused a decelerated tumor growth as compared with the unspecific control GbR201-H22(scFv) (**) and to the wild-type Gb-Ki4(scFv) (*). The difference between Gb-Ki4(scFv) and GbR201K-H22(scFv) was not significant (ns). (**c**) Confocal microscopy of Ki4(scFv)-SNAP-BG-Vista-Green (i) stained tissue sections of control-treated L428 tumors, Kat2 signal from transfected cells is visible in red (ii) and the overlay of an enlarged image.

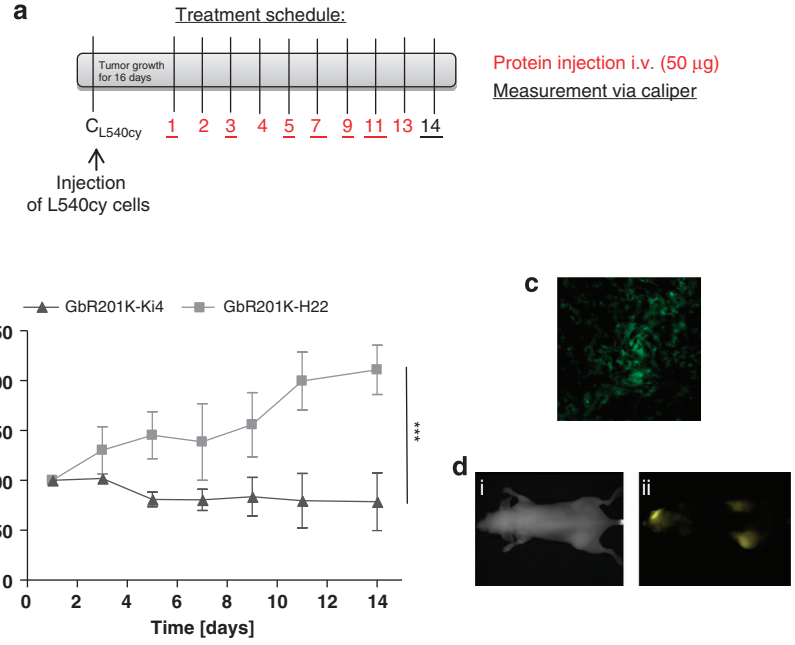

Figure 6. Results of mouse experiments with L540cy-induced tumors. (**a**) Treatment schedule indicating i.v. injection of cells, protein injection and days of measurement. (**b**) Relative tumor size is shown at time points as indicated upon treatment with mutant GbR201K-Ki4(scFv) versus control GbR201K-H22(scFv). The difference between the curves was determined to be statistically significant with $P < 0.001$ (***). (**c**) Confocal microscopy of Ki4(scFv)-SNAP-BG-Vista-Green-stained tissue sections of control-treated L540cy tumors. (**d**) Receptor depending targeting of L540cy with Ki4(scFv)-SNAP-BG-747 *in vivo* after 6 h. Protein was applied i.v. into L540cy-bearing mice. Measurement was taken with deep-red filter set ((730–950 nm) (i) background signal, (ii) image with fluorescence signal (yellow, Ki4(scFv)-SNAP-BG-747).

Staining of tissue sections cut from both L540cy and L428 tumors after excision confirmed the continued expression of CD30 after treatment with the Ki4(scFv)-derived constructs (Figures 5c and 6c). This excludes the reduction of CD30 by the tumor as mechanism to escape treatment. In addition, we confirmed CD30 receptor expression by the tumor cells *in vivo*. This was done using optical *in vivo* imaging, as described previously.[18,25] We injected Ki4(scFv)-SNAP-BG-747 into L540cy tumor-bearing mice, resulting in localization of the signal in the tumor only (Figure 6d).

In conclusion, we here for the first time in a proof-of-principle model demonstrate that residual therapy-resistant cancer cells can be killed when the resistance is due to PI-9 expression as escape mechanism. This was accomplished by a targeted immunotherapeutic approach comprising our novel GrB R201K variant, which kills these resistant, PI-9-positive cells in addition to PI-9-negative tumor cells. This finding is not just beneficial for HL treatment, but can also bear clinical relevance for the treatment of other hematological disorders, or solid tumors that potentially express PI-9 or selected PI-9-positive cells under immune surveillance or tumor therapy. As PI-9 expression correlates with an unfavorable clinical outcome, our targeted treatment approach using the here-described mutant GrBs may lead to specific elimination of these resistant cells, resulting in an improved therapeutic effect.

CONFLICT OF INTEREST

The authors declare no conflict of interest.

ACKNOWLEDGEMENTS

We gratefully acknowledge the excellent technical assistance of Anh-Tuan Pham during mouse experiments and of Sarah Kirchhoff during generation of mutants.

AUTHORSHIP CONTRIBUTIONS

SS, HPH and TT wrote the paper; SS and TT conceived, executed and analyzed the experiments. TT, MH and GH-T participated in planning and executing the animal experiments. RF and SB provided critical intellectual input and contributed to writing the manuscript.

REFERENCES

1 Mathew M, Verma RS. Humanized immunotoxins: a new generation of immunotoxins for targeted cancer therapy. *Cancer Sci* 2009; **100**: 1359–1365.
2 Kanatani I, Lin X, Yuan X, Manorek G, Shang X, Cheung LH *et al.* Targeting granzyme B to tumor cells using a yoked human chorionic gonadotropin. *Cancer Chemother Pharmacol* 2011; **68**: 979–990.
3 Kurschus FC, Fellows E, Stegmann E, Jenne DE. Granzyme B delivery via perforin is restricted by size, but not by heparan sulfate-dependent endocytosis. *Proc Natl Acad Sci USA* 2008; **105**: 13799–13804.
4 Kurschus FC, Jenne DE. Delivery and therapeutic potential of human granzyme B. *Immunol Rev* 2010; **235**: 159–171.
5 Liu Y, Cheung LH, Hittelman WN, Rosenblum MG. Targeted delivery of human pro-apoptotic enzymes to tumor cells: *in vitro* studies describing a novel class of recombinant highly cytotoxic agents. *Mol Cancer Ther* 2003; **2**: 1341–1350.
6 Stahnke B, Thepen T, Stocker M, Rosinke R, Jost E, Fischer R *et al.* Granzyme B-H22(scFv), a human immunotoxin targeting CD64 in acute myeloid leukemia of monocytic subtypes. *Mol Cancer Ther* 2008; **7**: 2924–2932.
7 Zhang L, Zhao J, Wang T, Yu CJ, Jia LT, Duan YY *et al.* HER2-targeting recombinant protein with truncated pseudomonas exotoxin A translocation domain efficiently kills breast cancer cells. *Cancer Biol Ther* 2008; **7**: 1226–1231.
8 Zhao J, Zhang LH, Jia LT, Zhang L, Xu YM, Wang Z *et al.* Secreted antibody/granzyme B fusion protein stimulates selective killing of HER2-overexpressing tumor cells. *J Biol Chem* 2004; **279**: 21343–21348.
9 Andrade F, Casciola-Rosen LA, Rosen A. Granzyme B-induced cell death. *Acta Haematol* 2004; **111**: 28–41.
10 Veugelers K, Motyka B, Goping IS, Shostak I, Sawchuk T, Bleackley RC. Granule-mediated killing by granzyme B and perforin requires a mannose 6-phosphate receptor and is augmented by cell surface heparan sulfate. *Mol Biol Cell* 2006; **17**: 623–633.
11 Jiang X, Ellison SJ, Alarid ET, Shapiro DJ. Interplay between the levels of estrogen and estrogen receptor controls the level of the granzyme inhibitor, proteinase inhibitor 9 and susceptibility to immune surveillance by natural killer cells. *Oncogene* 2007; **26**: 4106–4114.
12 van Houdt IS, Oudejans JJ, van den Eertwegh AJ, Baars A, Vos W, Bladergroen BA *et al.* Expression of the apoptosis inhibitor protease inhibitor 9 predicts clinical outcome in vaccinated patients with stage III and IV melanoma. *Clin Cancer Res* 2005; **11**: 6400–6407.
13 Soriano C, Mukaro V, Hodge G, Ahern J, Holmes M, Jersmann H *et al.* Increased proteinase inhibitor-9 (PI-9) and reduced granzyme B in lung cancer: mechanism for immune evasion? *Lung Cancer* 2012; **77**: 38–45.
14 Ray M, Hostetter DR, Loeb CR, Simko J, Craik CS. Inhibition of Granzyme B by PI-9 protects prostate cancer cells from apoptosis. *Prostate* 2012; **72**: 846–855.
15 Bladergroen BA, Meijer CJ, ten Berge RL, Hack CE, Muris JJ, Dukers DF *et al.* Expression of the granzyme B inhibitor, protease inhibitor 9, by tumor cells in patients with non-Hodgkin and Hodgkin lymphoma: a novel protective mechanism for tumor cells to circumvent the immune system? *Blood* 2002; **99**: 232–237.
16 ten Berge RL, Meijer CJ, Dukers DF, Kummer JA, Bladergroen BA, Vos W *et al.* Expression levels of apoptosis-related proteins predict clinical outcome in anaplastic large cell lymphoma. *Blood* 2002; **99**: 4540–4546.
17 Losasso V, Schiffer S, Barth S, Carloni P. Design of human granzyme B variants resistant to serpin B9. *Proteins* 2012; **80**: 2514–2522.
18 Pardo A, Stocker M, Kampmeier F, Melmer G, Fischer R, Thepen T *et al. In vivo* imaging of immunotoxin treatment using Katushka-transfected A-431 cells in a murine xenograft tumour model. *Cancer Immunol Immunother* 2012; **61**: 1617–1626.
19 Sun J, Whisstock JC, Harriott P, Walker B, Novak A, Thompson PE *et al.* Importance of the P4′ residue in human granzyme B inhibitors and substrates revealed by scanning mutagenesis of the proteinase inhibitor 9 reactive center loop. *J Biol Chem* 2001; **276**: 15177–15184.
20 Stocker M, Pardo A, Hetzel C, Reutelingsperger C, Fischer R, Barth S. Eukaryotic expression and secretion of EGFP-labeled annexin A5. *Protein Expr Purif* 2008; **58**: 325–331.
21 Barth S, Huhn M, Matthey B, Tawadros S, Schnell R, Schinkothe T *et al.* Ki-4(scFv)-ETA′, a new recombinant anti-CD30 immunotoxin with highly specific cytotoxic activity against disseminated Hodgkin tumors in SCID mice. *Blood* 2000; **95**: 3909–3914.
22 Edwards KM, Davis JE, Browne KA, Sutton VR, Trapani JA. Anti-viral strategies of cytotoxic T lymphocytes are manifested through a variety of granule-bound pathways of apoptosis induction. *Immuno Cell Biol* 1999; **77**: 76–89.
23 von Kalle C, Wolf J, Becker A, Sckaer A, Munck M, Engert A *et al.* Growth of Hodgkin cell lines in severely combined immunodeficient mice. *Int J Cancer* 1992; **52**: 887–891.
24 Hetzel C, Bachran C, Fischer R, Fuchs H, Barth S, Stocker M. Small cleavable adapters enhance the specific cytotoxicity of a humanized immunotoxin directed against CD64-positive cells. *J Immunother* 2008; **31**: 370–376.
25 Kampmeier F, Niesen J, Koers A, Ribbert M, Brecht A, Fischer R *et al.* Rapid optical imaging of EGF receptor expression with a single-chain antibody SNAP-tag fusion protein. *Eur J Nuc Med Mol Imaging* 2010; **37**: 1926–1934.
26 Klimka A, Matthey B, Roovers RC, Barth S, Arends JW, Engert A *et al.* Human anti-CD30 recombinant antibodies by guided phage antibody selection using cell panning. *Br J Cancer* 2000; **83**: 252–260.
27 Hansen HP, Recke A, Reineke U, Von Tresckow B, Borchmann P, Von Strandmann EP *et al.* The ectodomain shedding of CD30 is specifically regulated by peptide motifs in its cysteine-rich domains 2 and 5. *FASEB J* 2004; **18**: 893–895.
28 Younes A, Bartlett NL, Leonard JP, Kennedy DA, Lynch CM, Sievers EL *et al.* Brentuximab vedotin (SGN-35) for relapsed CD30-positive lymphomas. *N Engl J Med* 2010; **363**: 1812–1821.
29 Mahrus S, Kisiel W, Craik CS. Granzyme M is a regulatory protease that inactivates proteinase inhibitor 9, an endogenous inhibitor of granzyme B. *J Biol Chem* 2004; **279**: 54275–54282.
30 Classen CF, Bird PI, Debatin KM. Modulation of the granzyme B inhibitor proteinase inhibitor 9 (PI-9) by activation of lymphocytes and monocytes *in vitro* and by Epstein-Barr virus and bacterial infection. *Clin Exp Immunol* 2006; **143**: 534–542.
31 Tiacci E, Doring C, Brune V, van Noesel CJ, Klapper W, Mechtersheimer G *et al.* Analyzing primary Hodgkin and Reed-Sternberg cells to capture the molecular and cellular pathogenesis of classical Hodgkin lymphoma. *Blood* 2012; **120**: 4609–4620.
32 Gruss HJ, Boiani N, Williams DE, Armitage RJ, Smith CA, Goodwin RG. Pleiotropic effects of the CD30 ligand on CD30-expressing cells and lymphoma cell lines. *Blood* 1994; **83**: 2045–2056.
33 Krappmann D, Emmerich F, Kordes U, Scharschmidt E, Dorken B, Scheidereit C. Molecular mechanisms of constitutive NF-kappaB/Rel activation in Hodgkin/Reed-Sternberg cells. *Oncogene* 1999; **18**: 943–953.
34 Godal R, Keilholz U, Uharek L, Letsch A, Asemissen AM, Busse A *et al.* Lymphomas are sensitive to perforin-dependent cytotoxic pathways despite expression of PI-9 and overexpression of bcl-2. *Blood* 2006; **107**: 3205–3211.